# TEM4 is a junctional Rho GEF required for cell–cell adhesion, monolayer integrity and barrier function

**Siu P. Ngok[1], Rory Geyer[1], Antonis Kourtidis[1], Natalia Mitin[2], Ryan Feathers[1], Channing Der[2] and Panos Z. Anastasiadis[1,*]**

[1]Department of Cancer Biology, Mayo Clinic Comprehensive Cancer Center, Griffin Cancer Research Building, Room 307, 4500 San Pablo Road, Jacksonville, FL 32224, USA
[2]Department of Pharmacology, Lineberger Comprehensive Cancer Center, University of North Carolina at Chapel Hill, Chapel Hill, NC 27599, USA
*Author for correspondence (Anastasiadis.Panos@mayo.edu)

*Accepted 9 May 2013*
*Journal of Cell Science 126, 3271–3277*

*doi: 10.1242/jcs.123869*

## Summary

Signaling events mediated by Rho family GTPases orchestrate cytoskeletal dynamics and cell junction formation. The activation of Rho GTPases is tightly regulated by guanine-nucleotide-exchange factors (GEFs). In this study, we identified a novel Rho-specific GEF called TEM4 (tumor endothelial marker 4) that associates with multiple members of the cadherin–catenin complex and with several cytoskeleton-associated proteins. Depending on confluence, TEM4 localized to either actin stress fibers or areas of cell–cell contact. The junctional localization of TEM4 was independent of actin binding. Depletion of endogenous TEM4 by shRNAs impaired Madin–Darby canine kidney (MDCK) and human umbilical vein endothelial cell (HUVEC) cell junctions, disrupted MDCK acini formation in 3D culture and negatively affected endothelial barrier function. Taken together, our findings implicate TEM4 as a novel and crucial junctional Rho GEF that regulates cell junction integrity and epithelial and endothelial cell function.

**Key words:** TEM4, Cell junction, RhoA, Guanine nucleotide exchange factor, Cell adhesion, Catenin

## Introduction

The actin cytoskeleton is critical for cell–cell adhesion, cytokinesis, intracellular trafficking and cell motility (Hall, 1998; Etienne-Manneville and Hall, 2002). Rho GTPases are molecular binary switches that in their active GTP-loaded state regulate the assembly, disassembly and contractility of the cytoskeleton (Narumiya, 1996; Etienne-Manneville and Hall, 2002). In particular, RhoA directs the formation of actin stress fibers (Ridley and Hall, 1992; Chrzanowska-Wodnicka and Burridge, 1996); Rac1 promotes the assembly of lamellipodia and membrane ruffles (Ridley et al., 1992); and Cdc42 regulates the formation of filopodia (Nobes and Hall, 1995).

A number of recent reports support the hypothesis that the precise spatiotemporal activation of Rho GTPases by Rho GEFs (Rossman et al., 2005) is essential for modulating cytoskeletal events at the cell–cell junctions. For example, p114RhoGEF regulates apical contractility in epithelial cells by associating with circumferential myosin IIA (Nakajima and Tanoue, 2011; Terry et al., 2011). GEF-H1 mediates changes of actin and microtubule cytoskeleton to modulate cellular activities such as cytokinesis, cell cycle progression and paracellular permeability (Ren et al., 1998; Benais-Pont et al., 2003; Aijaz et al., 2005; Birkenfeld et al., 2007; Chang et al., 2008). Importantly, the specific activation of RhoA at intercellular junctions is critical for proper epithelial and endothelial junction formation and integrity (Terry et al., 2011; Ngok et al., 2012; Ratheesh et al., 2012). Despite these findings, the current understanding of the Rho-GEF–Rho signaling axis is limited. Rho GEFs outnumber their target GTPases by a factor of three. The role of many of these GEFs in the regulation of cytoskeletal dynamics, as well as their downstream effects on cell morphology and function are largely unknown.

To identify new regulators of Rho GTPases at cell junctions, we expressed a library of mammalian Rho GEFs in MDCK cells and screened it for junctional localization and for interaction with junctional proteins. We show that tumor endothelial marker 4 (TEM4; ARHGEF17) associates with the cadherin–catenin complex and localizes to areas of cell–cell contact in confluent cells. TEM4 is a Rho-specific GEF that contains an actin-binding domain (ABD), a Dbl homology (DH) domain and a pleckstrin homology (PH) domain (Fig. 1A) (Rümenapp et al., 2002; Mitin et al., 2012). shRNA-mediated knockdown of TEM4 in HUVECs and MDCK cells resulted in junctional defects and impaired cell morphology and monolayer function. We propose that TEM4 is a novel junctional Rho GEF essential for proper intercellular junction integrity and function in epithelial and endothelial cells.

## Results and Discussion

### TEM4 localizes to actin stress fibers in sparse cells and associates with components of the cytoskeleton

Previous work established the presence of an ABD at the N-terminus of TEM4 (Mitin et al., 2012). In agreement, GFP-tagged TEM4 colocalized with actin stress fibers when expressed in subconfluent MDCK cells (Fig. 1B). In contrast, a truncated variant of TEM4 lacking the entire N-terminal domain including the ABD, TEM4ΔN, exhibited cytoplasmic distribution (Fig. 1B). Using a commercial antibody, we were able to detect endogenous TEM4 by SDS-PAGE at the predicted 222 kDa molecular mass (Fig. 1C) both in epithelial (MDCK, Caco-2, Panc-1, UMRC3) and endothelial cells (HUVECs).

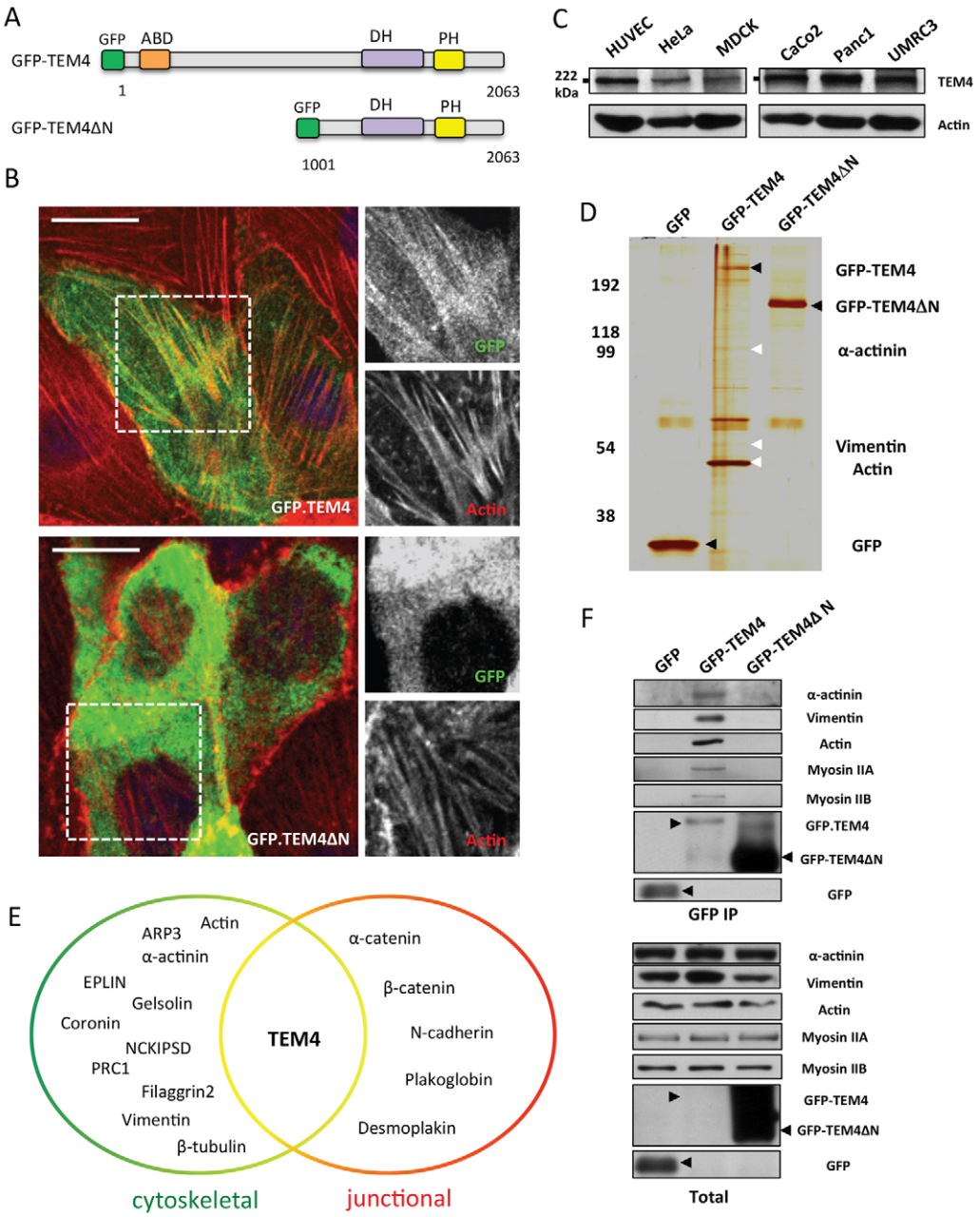


**Fig. 1. TEM4 associates with the cytoskeleton via its N-terminus.** (**A**) Schemes depicting GFP-tagged TEM4 and TEM4ΔN. ABD, actin-binding domain; DH, Dbl homology domain; PH, pleckstrin homology domain. (**B**) Immunofluorescence staining of GFP–TEM4 or GFP–TEM4ΔN and F-actin in MDCK cells. The framed region is shown separately to highlight the localization of expressed constructs. Scale bars: 20 µm. (**C**) Immunoblot analysis of TEM4 and actin in HUVEC, HeLa, MDCK, Caco-2, Panc1 and UMRC3 cells. (**D**) Silver staining of proteins co-immunoprecipitated with GFP–TEM4 in HeLa cells. (**E**) Scheme of putative TEM4-binding partners. TEM4 interacting partners are grouped as cytoskeleton or junction-associated proteins. (**F**) Co-immunoprecipitation analysis of TEM4-interacting partners.

Actin was shown previously to bind directly to TEM4 (Mitin et al., 2012). To identify additional TEM4 interacting partners, we expressed and immunoprecipitated GFP–TEM4 in HeLa cells and resolved and visualized the samples by SDS-PAGE and silver staining (Fig. 1D). Protein bands pulled down by GFP–TEM4 but not GFP (Fig. 1D, white arrows) were excised and subjected to mass spectrometry analysis (supplementary material Table S1) to identify potential interacting partners. Our analysis revealed that α-actinin, actin-related protein 3 (ARP3), gelsolin, flightless 1 homolog, epithelial protein lost in neoplasm (EPLIN), coronin 1C, filaggrin 2, vimentin and β-tubulin were present in the TEM4 immunoprecipitates in addition to actin (Fig. 1E). A number of these putative interactions, including interactions with actin, α-actinin and vimentin (as well as additional interactions with myosin IIA and IIB) were confirmed by co-immunoprecipitation experiments (Fig. 1F). As suggested by its inability to bind actin, TEM4ΔN did not interact with any of the cytoskeletal proteins associated with full length TEM4 (Fig. 1D,F).

### TEM4 associates with the cadherin–catenin complex and localizes to areas of cell–cell contact in confluent cells

In addition to cytoskeletal proteins, our proteomics analysis for TEM4 interacting partners revealed a large number of peptides related to the cadherin–catenin complex, including α-catenin, β-catenin, plakoglobin, N-cadherin and desmoplakin (supplementary material Table S1, Fig. 1E). The putative interactions with α- and β-catenin were further verified by co-immunoprecipitation experiments (Fig. 2A,B).

Based on these observations, we postulated that TEM4 is targeted to areas of cell–cell contact. To test this hypothesis, we cultured GFP–TEM4 expressing MDCK cells under conditions of confluence for 5 days to achieve cell polarization with distinct apical and basolateral regions. GFP–TEM4 localized to cell–cell contacts, whereas GFP–TEM4ΔN exhibited cytoplasmic distribution (Fig. 2C, GFP used as control), indicating that the N-terminal half of TEM4 is indispensable for junction localization. In addition, GFP–TEM4 co-localized with cortical actin and myosin IIB in MDCK cells, proteins associated with mature adherens junctions (supplementary material Fig. S1A–D). To assess whether TEM4 is targeted to cell–cell contacts through its association with actin proteins, we compared the intracellular localization of GFP–TEM4 with that of two actin-uncoupled TEM4 mutants – GFP–TEM4 R130D and GFP–TEM4Δ125–135 (supplementary material Fig. S2) (Mitin et al., 2012). When expressed in confluent MDCK cells, both TEM4 mutants retained their junctional localization (Fig. 2D), indicating that the recruitment of TEM4 to cell–cell contacts is independent of its

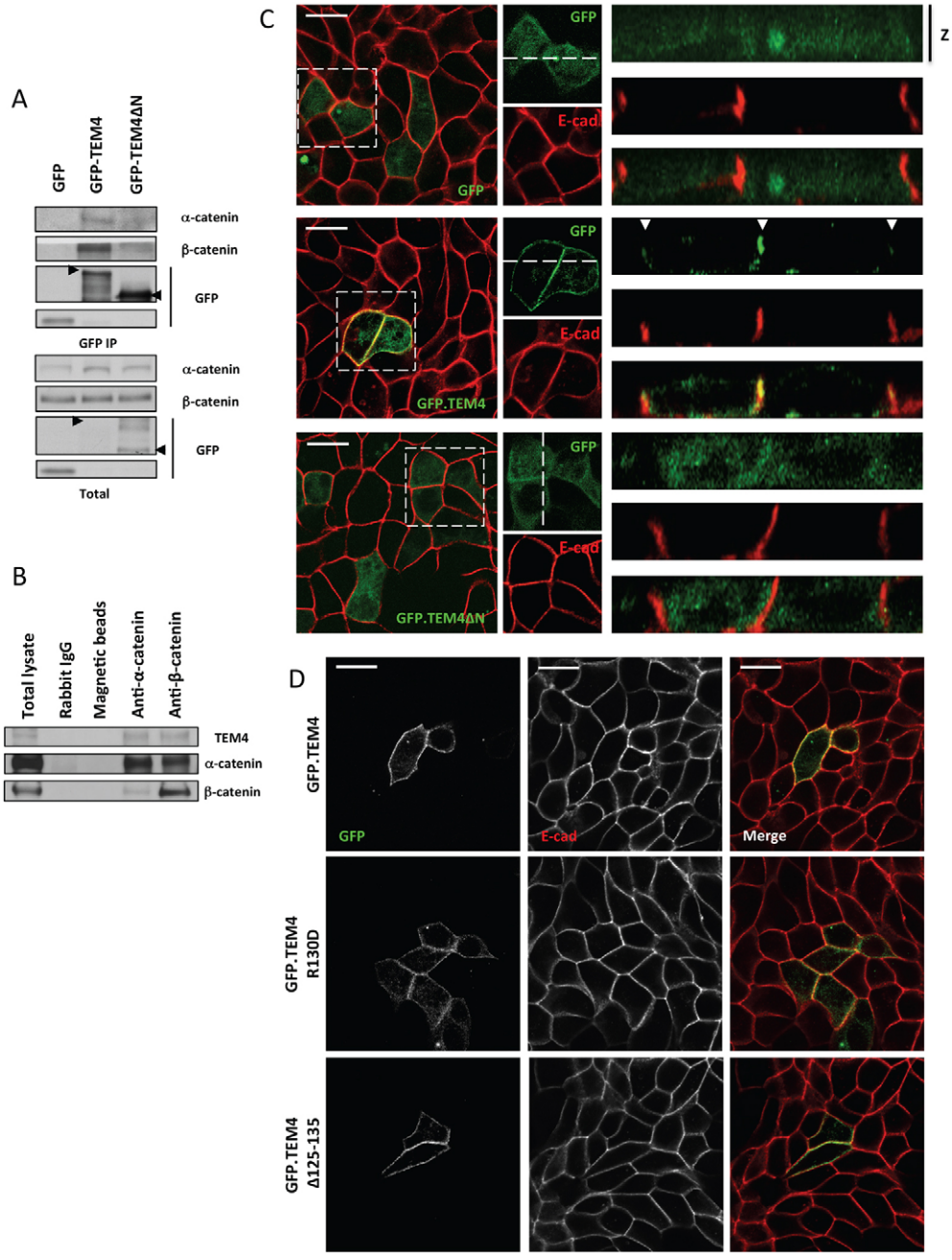


**Fig. 2. TEM4 localization to areas of cell–cell contact is independent of actin association.** (**A**) Co-immunoprecipitation analysis showing α-catenin and β-catenin as additional binding partners of GFP–TEM4. (**B**) Co-immunoprecipitation analysis showing endogenous TEM4 in α-catenin and β-catenin immunoprecipitates from polarized MDCK cells. (**C**) Immunofluorescence staining of GFP, GFP–TEM4, or GFP–TEM4ΔN together with E-cadherin in polarized MDCK cells. Transfected cells were plated at high density and cultured for 5 days. The framed region is shown separately to highlight the localization of expressed constructs. Vertical images (*z* section) highlight the junctional localization of GFP–TEM4 (arrowheads) but not GFP or GPF–TEM4ΔN. Scale bars: 20 µm. (**D**) Immunofluorescence staining of GFP–TEM4, GFP–TEM4 R130D or GFP–TEM4 Δ124–135, and E-cadherin in polarized MDCK cells. Transfected cells were seeded at high density and cultured for 5 days. Note that both actin-uncoupled TEM4 mutants (R130D and Δ124-135) still retain prominent junctional staining. Scale bars: 20 µm.

ability to bind actin and likely depends on its association with components of the cadherin–catenin complex. Combined, the data suggest that TEM4 is a new member of the cadherin–catenin complex at mature cell junctions.

### Downregulation of TEM4 alters MDCK cell morphology and acini morphogenesis

To determine the physiological significance of TEM4, we initially investigated whether downregulation of TEM4 has an effect on MDCK cell morphology. Depletion of TEM4 by either of two non-overlapping, canine-specific shRNAs markedly reduced TEM4 expression (Fig. 3A) and altered the overall morphology of MDCK cells. Compared to the cuboidal shape of control cells, silencing TEM4 resulted in an elongated and spindle-like phenotype (Fig. 3B). Unlike control cells that polarized properly, TEM4-depleted cells exhibited a disorganized monolayer morphology (Fig. 3C). Consistent with this, the localization of cortical actin, afadin, myosin IIA and myosin IIB to the junctions of TEM-4-depleted cells was disrupted (supplementary material Fig. S3A), suggesting that mature cell junctions were compromised. Importantly, downregulation of TEM4 reduced RhoA activity and myosin light chain 2 (MLC2) phosphorylation (Fig. 3D), which could account for the disorganized morphology observed (Fig. 3B,C) by disrupting apical contractility. Despite the reduced accumulation of other mature junction components, E-cadherin and β-catenin were retained at areas of cell–cell contact, which were more spread and disorganized, consistent with a loss of apical tension (supplementary material Fig. S3B). Finally, the observed effects of TEM-4 depletion were not mediated by altered protein levels of E-cadherin, β-catenin, afadin, myosin IIA or myosin IIB (supplementary material Fig. S4A).

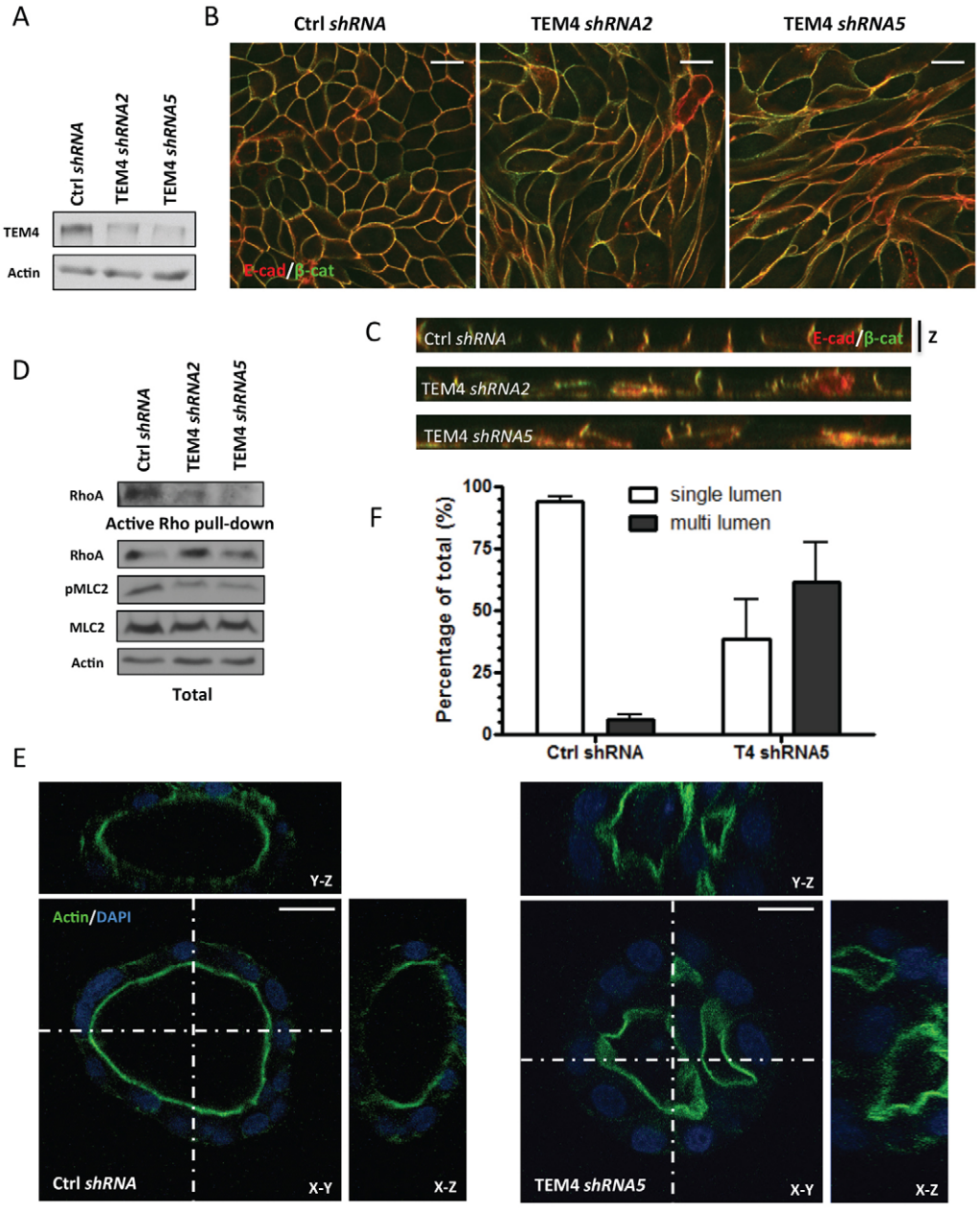


**Fig. 3. TEM4 is important for epithelial cell junction and proper acini formation.** (**A**) At 4 days post infection, MDCK cells expressing the indicated canine-specific shRNA were lysed and subjected to immunoblot analysis for TEM4 and actin. (**B**) Immunofluorescence staining of E-cadherin and β-catenin in the same set of cells as in A. Cells were plated at high density and cultured for 5 days. Scale bars: 20 µm. (**C**) Vertical images (*z* section) of B showing disrupted monolayer morphology in TEM4-depleted cells. (**D**) Immunoblot analysis of active RhoA and phosphorylated (pSer19) myosin light chain 2 (pMLC2) in MDCK cells expressing the indicated canine-specific shRNA. (**E**) Immunofluorescence staining of F-actin and nuclei (DAPI) in MDCK acini expressing the indicated shRNA. The lines correspond to the *x-z* and *y-z* sections. Scale bars: 20 µm. (**F**) Quantification of single versus multi-lumen acini in D, presented as a percentage of the total (mean ± s.e., $n=3$, 50 acini analyzed per condition per experiment).

Since cell shape and apical contractility are closely correlated with the coordination of cell polarity and tissue remodeling (Mège et al., 2006; Baum and Georgiou, 2011), we hypothesized that the depletion of TEM4 interferes with the ability of MDCK cells to form polarized single-lumen acini in 3D cell culture. Indeed, TEM4 downregulation resulted in a significant increase in the formation of multi-lumen acini, as assessed by immunofluorescence staining of F-actin (Fig. 3E,F). Despite a more diffused and less linear actin organization, the apical localization of actin was preserved (Fig. 3E), suggesting that TEM4 depletion does not affect directly epithelial cell polarization.

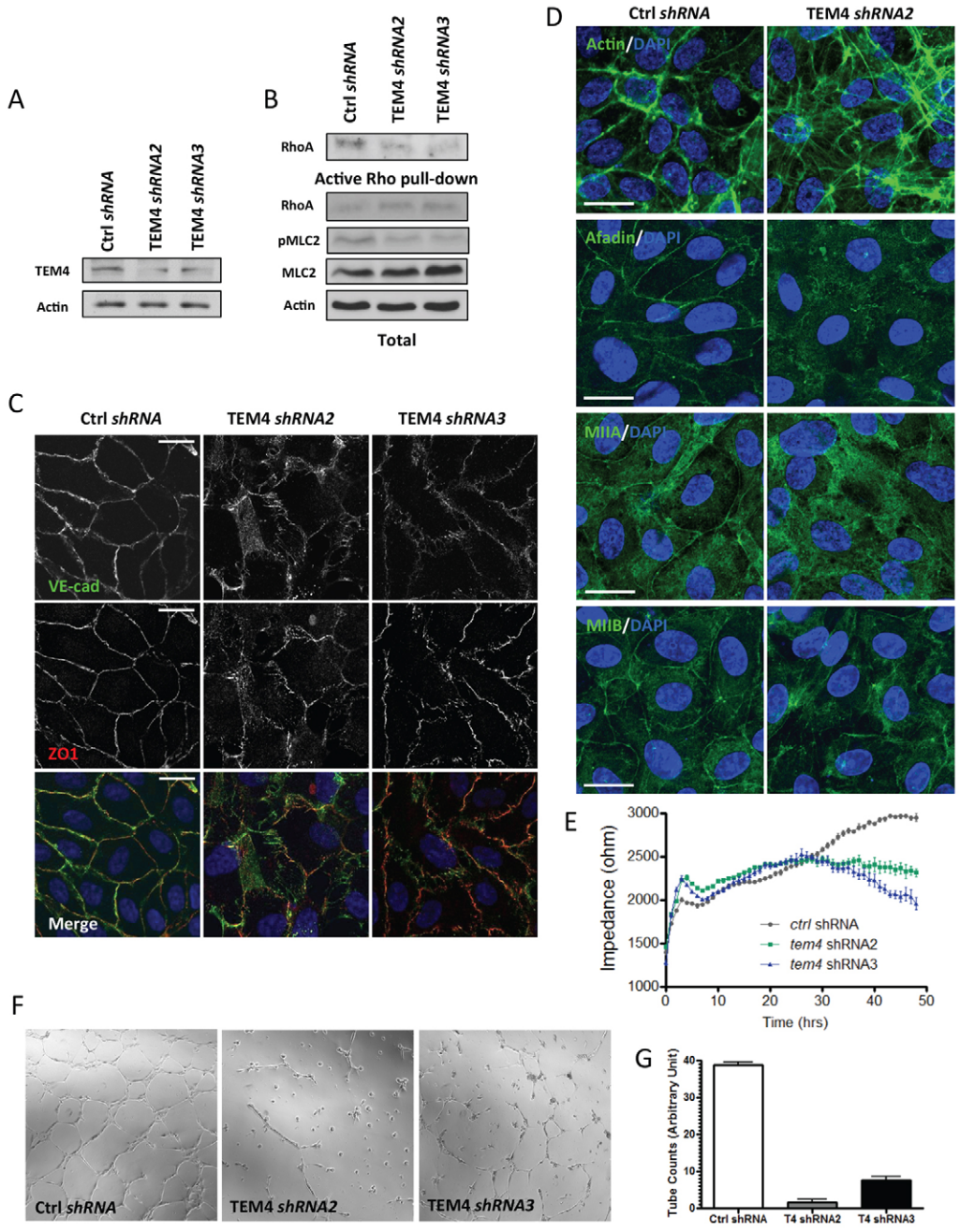


**Fig. 4. TEM4 plays a role in endothelial monolayer patency and barrier function.** (**A**) At 4 days post infection, HUVECs expressing the indicated human-specific shRNA were lysed and subjected to immunoblot analysis for TEM4 and actin. (**B**) Immunoblot analysis of active RhoA and phosphorylated (pSer19) MLC2 (pMLC2) in HUVECs expressing the indicated human-specific shRNA. (**C**) Immunofluorescence staining of VE-cadherin and ZO1 in HUVECs expressing the same set of shRNAs as in A. Scale bars: 20 µm. (**D**) Immunofluorescence staining of F-actin, afadin, myosin IIA and myosin IIB in HUVECs expressing the indicated shRNA. Scale bars: 20 µm. (**E**) Impedance measurement of quiescent HUVEC monolayers. HUVECs expressing the indicated shRNA were plated on ECIS electrode arrays; impedance at 4000 Hz was recorded every 180 seconds for 48 hours (mean ± s.e.). Results are representative of three independent experiments performed in quadruplicate. (**F**) Representative phase-contrast images of *in vitro* angiogenesis assays performed using shRNA-expressing HUVECs. (**G**) Quantification of the number of tubes in D (mean ± s.e., $n=3$, four fields per condition analyzed per experiment).

### Depletion of TEM4 leads to defective endothelial cell junctions and attenuated *in vitro* angiogenesis

As TEM4 belongs to a family of markers identified in the vasculature (St Croix et al., 2000), we asked whether it is important for endothelial junctions and barrier function. Two non-overlapping human-specific TEM4 shRNAs were used to downregulate TEM4 expression in HUVECs (Fig. 4A). Similar to MDCK cells, silencing TEM4 in HUVECs reduced RhoA activity and MLC2 phosphorylation (Fig. 4B) without altering the protein levels of junctional and cytoskeletal components (supplementary material Fig. S4B). Furthermore, TEM4 depletion resulted in disorganized staining of both VE-cadherin and ZO1 (Fig. 4C), key markers of endothelial junction integrity. The distribution of afadin, myosin IIA and myosin IIB at areas of cell–cell contact were disrupted in TEM4-depleted HUVECs and the circumferential actin belt was absent (Fig. 4D). Next, we investigated the functional consequence of TEM4 downregulation by measuring the barrier function of confluent, growth-arrested HUVECs using the Electric Cell-substrate Impedance System (ECIS). Compared to the trans-endothelial impedance of control cells, which climbed steadily and plateaued at around 48 hours, the impedance of TEM4-depleted cells plateaued at a much earlier time point and the end-point readout was significantly lower (Fig. 4E). Using a transwell permeability assay, increased leakage of fluorescence tracer through the barrier of TEM4-depleted cells was detected (data not shown). These observations strongly suggest that TEM4 is necessary for junction maturity and the formation of a patent endothelial monolayer.

Using an *in vitro* angiogenesis assay, we then assessed the endothelial function of control versus TEM4-depleted HUVECs. TEM4 depletion abrogated the capability of cells to branch out and form two-dimensional, tube-like structures when plated on top of matrigel (Fig. 4F,G). The inability of these cells to form a branched network by making contact with neighboring cells is consistent with the observed defects in cell adhesion (Fig. 4C,D). In addition, tube formation of endothelial cells in culture requires the establishment of polarized, directed cell migration (Egginton and Gerritsen, 2003), suggesting that TEM4 may play a role in endothelial cell migration.

Altogether, TEM4 depletion-induced phenomena in endothelial cells mirror those seen in epithelial cells. Based on our findings, we propose that TEM4 is a novel junction-associated Rho GEF that plays a critical role in regulating cell adhesion, monolayer integrity and barrier function. Previous studies have indicated that the Rho-specific GEFs p114RhoGEF and Ect2 (in epithelial cells) (Terry et al., 2011; Ratheesh et al., 2012), as well as Syx (in endothelial cells) are required for intercellular junction integrity by locally activating RhoA at the junctions (Ngok et al., 2012). We postulate that TEM4 also activates RhoA locally to modulate junction contractility and stability. The observation that more than one Rho-specific GEFs are involved in junction function in either MDCK cells or HUVECs implies non-overlapping functions for these Rho GEFs and suggests that RhoA activation is required at multiple steps during junction formation, maturation and maintenance.

Finally, a point mutation in TEM4 that results in a premature termination codon has been identified in mucosal melanoma (Bloethner et al., 2008), raising the possibility that mutation of TEM4 may contribute to tumorigenicity.

## Materials and Methods

#### Cell culture and transfection

HeLa and MDCK cells were cultured in DMEM (Cellgro) containing 10% fetal bovine serum (Invitrogen) and transfected with TransIT-HeLaMonster (Mirus) or Lipofectamine 2000 (Invitrogen). HUVECs were cultured in EGM-2 (Lonza).

Acini were grown as reported previously (Wang et al., 1990). Briefly, $4\times10^3$ MDCK cells were re-suspended in 2% matrigel/media mixture and plated on 100% matrigel (BD Bioscience) in an 8-well chamber slide. Cells were re-fed with fresh matrigel/media every 2 days and cultured for 7 days.

#### DNA constructs, antibodies and reagents

pEGFP-TEM4, pEGFP-TEM4ΔN, pEGFP-TEM4 R130D and pEGFP-TEM4 Δ125-135 have been described previously (Mitin et al., 2012). Primary antibodies used were: rabbit anti-TEM4 (Novus); mouse anti-E-cadherin, anti-vimentin (BD Bioscience); rabbit anti-MLC2, anti-pSer19 MLC2 (Cell Signaling); mouse anti-GFP 3E6, anti-p120 (15D2), mouse and rabbit anti-ZO1 (Invitrogen); rabbit anti-Myosin IIA, anti-Myosin IIB (Covance); mouse anti-RhoA, rabbit anti-α-actinin (Santa Cruz); rabbit anti-α-catenin, anti-β-catenin, anti-actin, anti-afadin (Sigma-Aldrich); mouse anti-VE-cadherin (Millipore). Phalloidin (Invitrogen) was used to stain F-actin. Silver Staining Kit for Mass Spectrometry was purchased from Pierce.

#### Immunofluorescence, immunoprecipitation and immunoblotting

Immunofluorescence: cells seeded on cover glass, collagen-coated coverslips, or matrigel were fixed with methanol or 3% paraformaldehyde as previously reported (Anastasiadis et al., 2000) and probed with primary antibodies followed by incubation with Alexa Fluor secondary antibodies (Invitrogen). Images were acquired with a Zeiss LSM 510 META confocal microscope.

Immunoprecipitation: protein G beads (Invitrogen) were conjugated with anti-GFP (Invitrogen), α-catenin or β-catenin (Sigma-Aldrich) antibody. Cells were lysed with TritonX buffer (50 mM Tris, 150 mM NaCl, 1 mM EDTA, 1% Triton X, pH 7.4). Cleared lysates were incubated with prepared beads and washed with lysis buffer. Bound proteins were eluted by boiling in 2×LSB.

Immunoblotting: protein samples were resolved with SDS-PAGE, transferred to nitrocellulose membrane and probed with primary and peroxidase-conjugated secondary antibodies (Jackson ImmunoResearch). Bands were detected using ECL (GE Healthcare).

#### Rho activity assay

The level of activated RhoA was determined in cells using rhotekin pull-down assays as previously described (Ngok et al., 2013). Briefly, cells (HUVECs, MDCK and HeLa) were grown to confluence in 6 cm plates and lysed with Rho activity lysis buffer (20 mM HEPES, 100 mM NaCl, 10% glycerol, 0.5% NP40, 0.2% deoxycholic acid, 100 mM $MgCl_2$, pH 7.5); cell lysates were collected and cleared by centrifugation, the supernatants were then incubated with reconstituted GST-fused rhotekin-RBD protein beads (Cytoskeleton) at 4℃ for 45 minutes, beads were washed three times with the lysis buffer and bound proteins were eluted by boiling in loading buffer.

#### shRNA lentivirus production

Lentiviral vectors (pLKO) encoding non-target shRNA along with human specific shRNAs targeting TEM4 were purchased from Open Biosystems (shRNA2, NM_014786.2-2407s1c1; shRNA3, NM_014786.2-2902s1c1). Canine-specific shRNAs were designed using human shRNAs as templates. The specific sequences were: canine shRNA2, 5′-GAGGTTATTCAGAGTATTGTT-3′; canine shRNA5, 5′-GTATCTGAATAACCAGGTGTT-3′.

Lentivirus was produced as reported previously (Lewis-Tuffin et al., 2010). Briefly, 293FT cells were transfected with virapower packaging mix (Invitrogen) and lentiviral vectors using Lipofectamine 2000. MDCK cells and HUVECs were infected using polybrene (Sigma-Aldrich) and selected for 2 days with puromycin.

#### Impedance measurement of endothelial barrier function

ECIS Z (Electric Cell-substrate Impedance System, Applied Biophysics) was used to measure the trans-endothelial impedance of HUVEC monolayers. $1\times10^5$ HUVECs were plated on Electrode Arrays (8W10E, Applied Biophysics) and maintained for 48 hours. Impedance measurement (4000 Hz) was taken every 180 seconds for the duration of the experiment. Each condition was performed in quadruplicate.

#### *In vitro* angiogenesis/tube formation assay

HUVECs were re-suspended in EGM-2 media and seeded at the appropriate density on an 8-well chamber containing 100% Matrigel (BD Bioscience). Phase-contrast images were acquired 12 hours post seeding. Tube formation was assessed by manual counting.

## Acknowledgements

We thank Ben Madden and the Mayo Proteomics Research Center for their assistance with Mass Spectrometry analysis.

## Author contibutions

S.P.N., R.G., R.F. and A.K. performed the experiments; S.P.N. and P.Z.A. designed and analyzed the experiments; N.M. and C.D. provided reagents; S.P.N. and P.Z.A. wrote the manuscript; A.K., N.M. and C.D. corrected the manuscript.

## Funding

The work was supported by the National Institutes of Health [grant numbers R01 NS069753, R21 NS070117 to P.Z.A.]; and the Mayo Graduate School (to S.P.N.). Deposited in PMC for release after 12 months.

Supplementary material available online at
http://jcs.biologists.org/lookup/suppl/doi:10.1242/jcs.123869/-/DC1

## References

**Aijaz, S., D'Atri, F., Citi, S., Balda, M. S. and Matter, K.** (2005). Binding of GEF-H1 to the tight junction-associated adaptor cingulin results in inhibition of Rho signaling and G1/S phase transition. *Dev. Cell* **8**, 777-786.

**Anastasiadis, P. Z., Moon, S. Y., Thoreson, M. A., Mariner, D. J., Crawford, H. C., Zheng, Y. and Reynolds, A. B.** (2000). Inhibition of RhoA by p120 catenin. *Nat. Cell Biol.* **2**, 637-644.

**Baum, B. and Georgiou, M.** (2011). Dynamics of adherens junctions in epithelial establishment, maintenance, and remodeling. *J. Cell Biol.* **192**, 907-917.

**Benais-Pont, G., Punn, A., Flores-Maldonado, C., Eckert, J., Raposo, G., Fleming, T. P., Cereijido, M., Balda, M. S. and Matter, K.** (2003). Identification of a tight junction-associated guanine nucleotide exchange factor that activates Rho and regulates paracellular permeability. *J. Cell Biol.* **160**, 729-740.

**Birkenfeld, J., Nalbant, P., Bohl, B. P., Pertz, O., Hahn, K. M. and Bokoch, G. M.** (2007). GEF-H1 modulates localized RhoA activation during cytokinesis under the control of mitotic kinases. *Dev. Cell* **12**, 699-712.

**Bloethner, S., Mould, A., Stark, M. and Hayward, N. K.** (2008). Identification of ARHGEF17, DENND2D, FGFR3, and RB1 mutations in melanoma by inhibition of nonsense-mediated mRNA decay. *Genes Chromosomes Cancer* **47**, 1076-1085.

**Chang, Y. C., Nalbant, P., Birkenfeld, J., Chang, Z. F. and Bokoch, G. M.** (2008). GEF-H1 couples nocodazole-induced microtubule disassembly to cell contractility via RhoA. *Mol. Biol. Cell* **19**, 2147-2153.

**Chrzanowska-Wodnicka, M. and Burridge, K.** (1996). Rho-stimulated contractility drives the formation of stress fibers and focal adhesions. *J. Cell Biol.* **133**, 1403-1415.

**Egginton, S. and Gerritsen, M.** (2003). Lumen formation: in vivo versus in vitro observations. *Microcirculation* **10**, 45-61.

**Etienne-Manneville, S. and Hall, A.** (2002). Rho GTPases in cell biology. *Nature* **420**, 629-635.

**Hall, A.** (1998). Rho GTPases and the actin cytoskeleton. *Science* **279**, 509-514.

**Lewis-Tuffin, L. J., Rodriguez, F., Giannini, C., Scheithauer, B., Necela, B. M., Sarkaria, J. N. and Anastasiadis, P. Z.** (2010). Misregulated E-cadherin expression associated with an aggressive brain tumor phenotype. *PLoS ONE* **5**, e13665.

**Mège, R. M., Gavard, J. and Lambert, M.** (2006). Regulation of cell-cell junctions by the cytoskeleton. *Curr. Opin. Cell Biol.* **18**, 541-548.

**Mitin, N., Rossman, K. L. and Der, C. J.** (2012). Identification of a novel actin-binding domain within the Rho guanine nucleotide exchange factor TEM4. *PLoS ONE* **7**, e41876.

**Nakajima, H. and Tanoue, T.** (2011). Lulu2 regulates the circumferential actomyosin tensile system in epithelial cells through p114RhoGEF. *J. Cell Biol.* **195**, 245-261.

**Narumiya, S.** (1996). The small GTPase Rho: cellular functions and signal transduction. *J. Biochem.* **120**, 215-228.

**Ngok, S. P., Geyer, R., Liu, M., Kourtidis, A., Agrawal, S., Wu, C., Seerapu, H. R., Lewis-Tuffin, L. J., Moodie, K. L., Huveldt, D. et al.** (2012). VEGF and Angiopoietin-1 exert opposing effects on cell junctions by regulating the Rho GEF Syx. *J. Cell Biol.* **199**, 1103-1115.

**Ngok, S. P., Geyer, R., Kourtidis, A., Storz, P. and Anastasiadis, P. Z.** (2013). Phosphorylation-mediated 14-3-3 protein binding regulates the function of the rho-specific guanine nucleotide exchange factor (RhoGEF) Syx. *J. Biol. Chem.* **288**, 6640-6650.

**Nobes, C. D. and Hall, A.** (1995). Rho, rac, and cdc42 GTPases regulate the assembly of multimolecular focal complexes associated with actin stress fibers, lamellipodia, and filopodia. *Cell* **81**, 53-62.

**Ratheesh, A., Gomez, G. A., Priya, R., Verma, S., Kovacs, E. M., Jiang, K., Brown, N. H., Akhmanova, A., Stehbens, S. J. and Yap, A. S.** (2012). Centralspindlin and α-catenin regulate Rho signalling at the epithelial zonula adherens. *Nat. Cell Biol.* **14**, 818-828.

**Ren, Y., Li, R., Zheng, Y. and Busch, H.** (1998). Cloning and characterization of GEF-H1, a microtubule-associated guanine nucleotide exchange factor for Rac and Rho GTPases. *J. Biol. Chem.* **273**, 34954-34960.

**Ridley, A. J. and Hall, A.** (1992). The small GTP-binding protein rho regulates the assembly of focal adhesions and actin stress fibers in response to growth factors. *Cell* **70**, 389-399.

**Ridley, A. J., Paterson, H. F., Johnston, C. L., Diekmann, D. and Hall, A.** (1992). The small GTP-binding protein rac regulates growth factor-induced membrane ruffling. *Cell* **70**, 401-410.

**Rossman, K. L., Der, C. J. and Sondek, J.** (2005). GEF means go: turning on RHO GTPases with guanine nucleotide-exchange factors. *Nat. Rev. Mol. Cell Biol.* **6**, 167-180.

**Rümenapp, U., Freichel-Blomquist, A., Wittinghofer, B., Jakobs, K. H. and Wieland, T.** (2002). A mammalian Rho-specific guanine-nucleotide exchange factor (p164-RhoGEF) without a pleckstrin homology domain. *Biochem. J.* **366**, 721-728.

**St Croix, B., Rago, C., Velculescu, V., Traverso, G., Romans, K. E., Montgomery, E., Lal, A., Riggins, G. J., Lengauer, C., Vogelstein, B. et al.** (2000). Genes expressed in human tumor endothelium. *Science* **289**, 1197-1202.

**Terry, S. J., Zihni, C., Elbediwy, A., Vitiello, E., Leefa Chong San, I. V., Balda, M. S. and Matter, K.** (2011). Spatially restricted activation of RhoA signalling at epithelial junctions by p114RhoGEF drives junction formation and morphogenesis. *Nat. Cell Biol.* **13**, 159-166.

**Wang, A. Z., Ojakian, G. K. and Nelson, W. J.** (1990). Steps in the morphogenesis of a polarized epithelium. I. Uncoupling the roles of cell-cell and cell-substratum contact in establishing plasma membrane polarity in multicellular epithelial (MDCK) cysts. *J. Cell Sci.* **95**, 137-151.

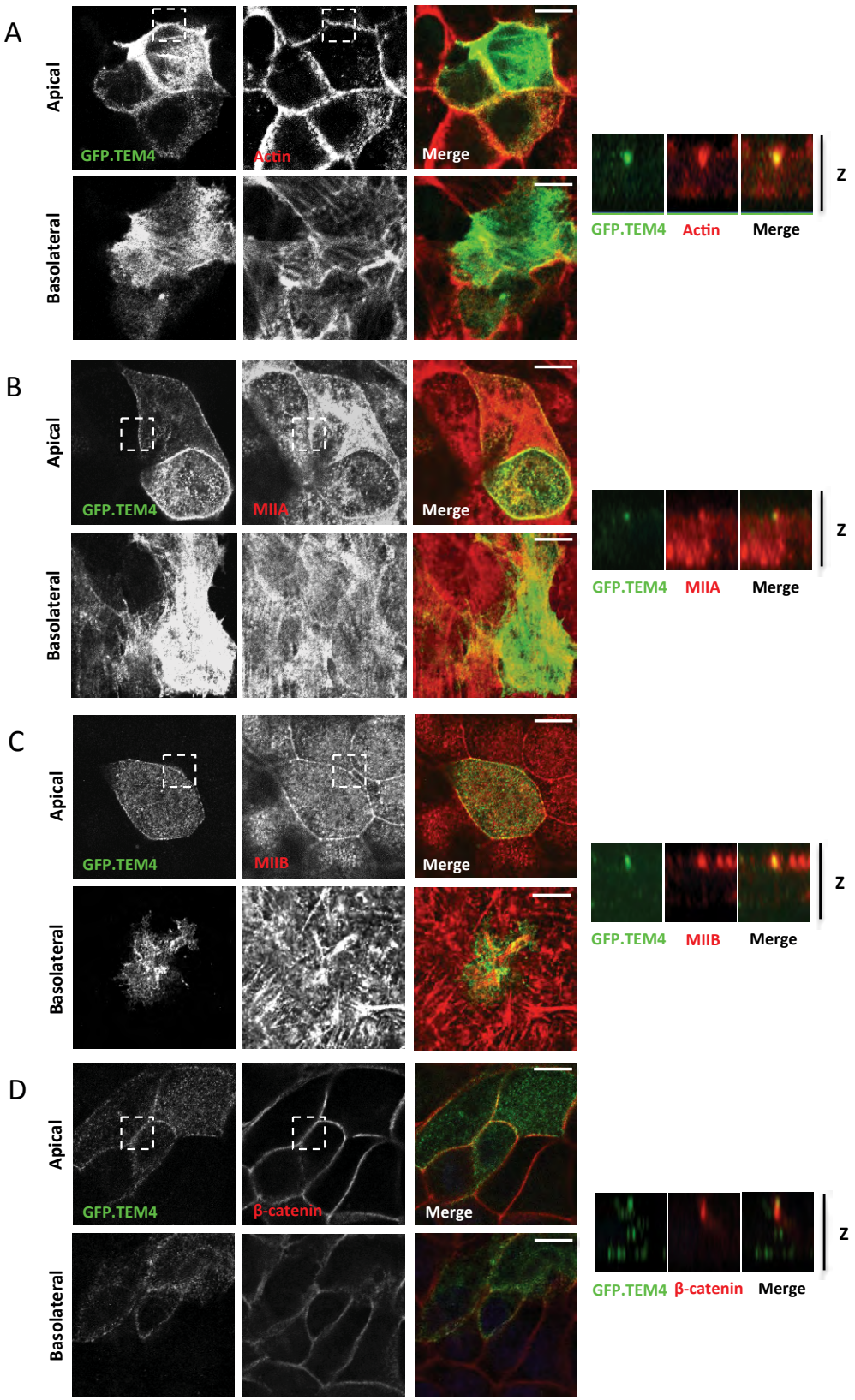


**Fig. S1. TEM4 co-localizes with identified binding partners in MDCK cells.** (A-D) Immunofluorescence staining of GFP-TEM4, F-actin, myosin IIA, myosin IIB, and β-catenin in MDCK cells. Transfected cells were seeded at high density and cultured for 5 days prior to fixation and imaging. Each set of images (z-stack) represents a single field, with one apical and one basolateral image shown. The framed regions correspond to the vertical images (Z section) that are shown on the right and highlight the co-localization. Bars, 10μm.

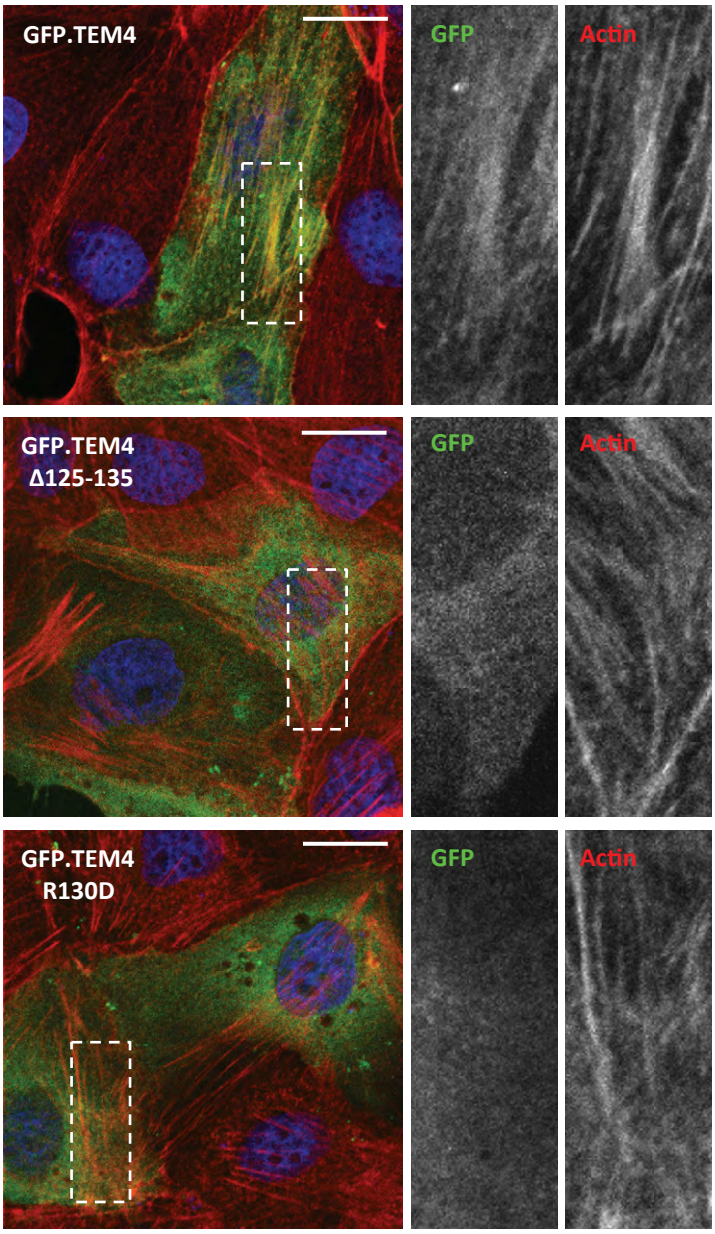


**Fig. S2. Actin-uncoupled TEM4 R130D and TEM4 Δ125-135 mutants do not co-localize with the actin cytoskeleton in sub-confluent MDCK cells.** Immunofluorescence staining of GFP-TEM4, GFP-TEM4 R130D, or GFP-TEM4Δ124-135 and F-actin in sub-confluent MDCK cells. The framed region is shown separately to highlight the localization of expressed constructs. Bars, 20µm.

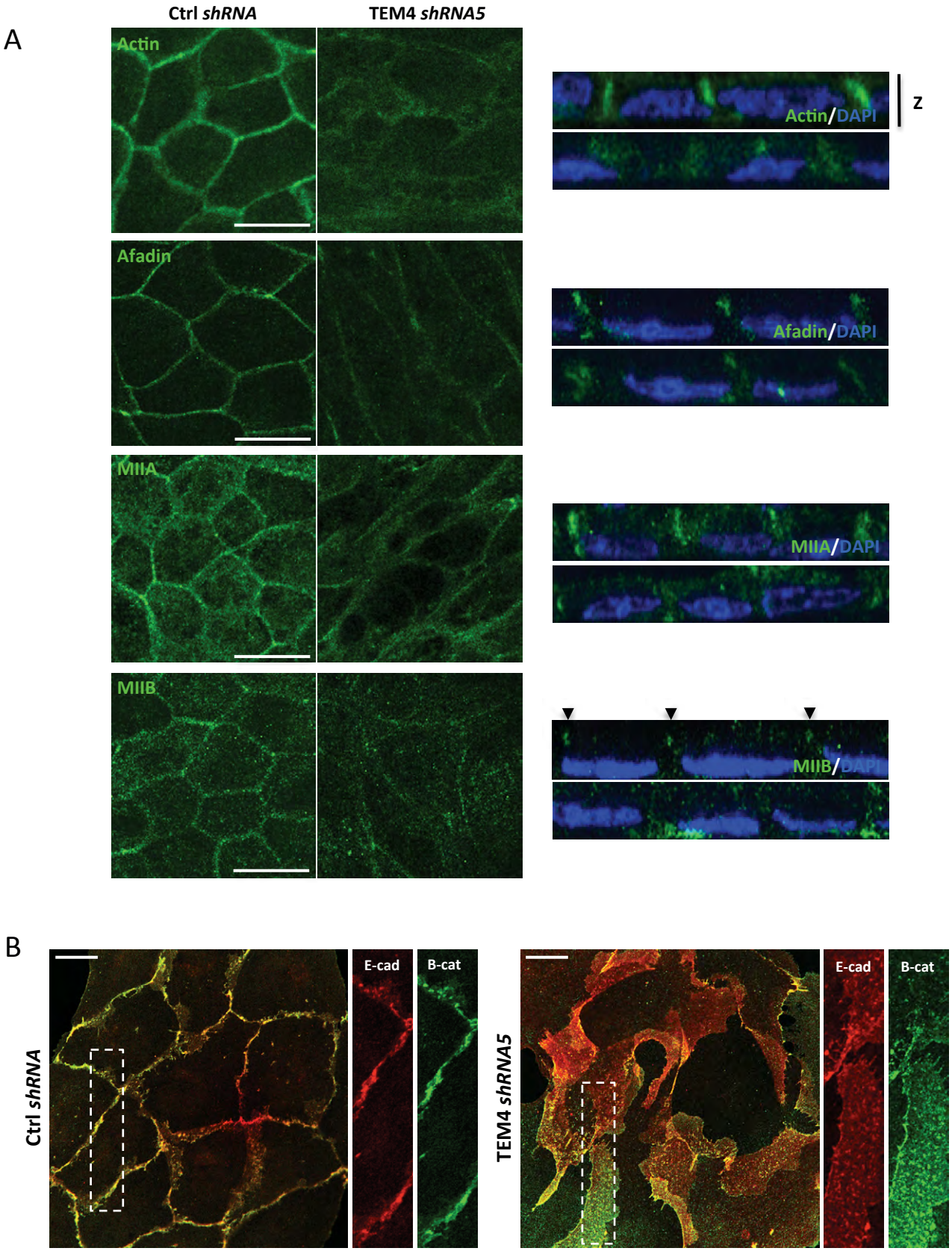


**Fig. S3. Silencing TEM4 disrupts normal MDCK cell morphology.** (A) Immunofluorescence staining of F-actin, afadin, myosin IIA, and myosin IIB in MDCK cells expressing the indicated shRNA. Cells were plated at high density and cultured for 5 days. Vertical images (Z section) show disorganized distribution of the indicated protein in TEM4-depleted cells compared to their control counterparts. Arrows highlight apically localized myosin IIB in control cells. Bars, 20µm. (B) Immunofluorescence staining of E-cadherin and β-catenin in MDCK cells expressing the indicated shRNA. The framed region is shown separately to highlight differences in the localization of E-cadherin and β-catenin in these cells. Bars, 20µm.

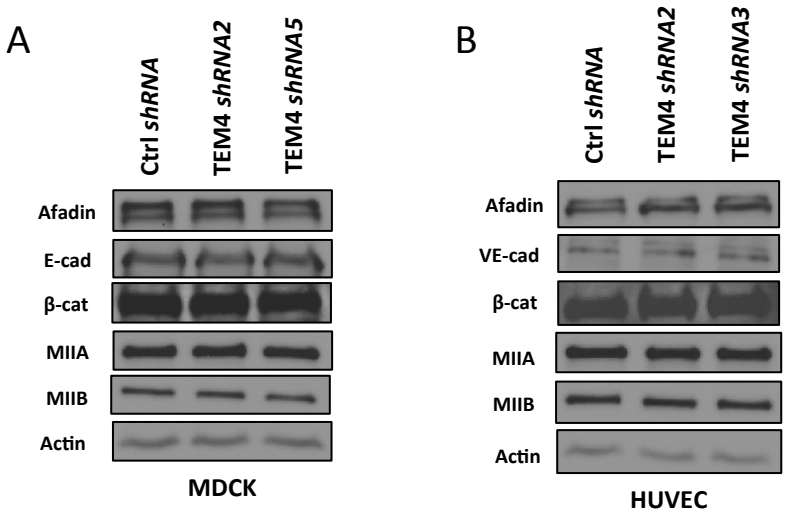


**Fig. S4. TEM4 depletion does not affect junctional and cytoskeletal protein stability.** (A-B) Immunoblot analysis of afadin, E- or VE-cadherin, β-catenin, myosin IIA, and myosin IIB in MDCK cells and HUVECs expressing the indicated TEM4 shRNA.

| Name | Alias | Accession | Predicted Size (kDa) | Peptide Count |
|---|---|---|---|---|
| TEM4 | ARHGEF17, p164RhoGEF | NP_055601 | 224 | 151 |
| β-catenin | CTNNB1 | NP_001895 | 86 | 119 |
| α-catenin | CTNNA1 | NP_001894 | 101 | 176 |
| Vimentin | VIM | NP_003371 | 54 | 159 |
| Desmoplakin | DSP | NP_004406 | 334 | 59 |
| Plakoglobin | JUP | NP_068831 | 82 | 186 |
| N-cadherin | CDH2 | NP_001783 | 100 | 39 |
| α-actinin-4 | ACTN4 | NP_004915 | 103 | 88 |
| α-actinin-1 | ACTN1 | NP_001093 | 103 | 83 |
| Actin-related protein 3 | ARP3 | NP_005712 | 48 | 48 |
| Filaggrin 2 | FLG2 | NP_001014364 | 249 | 9 |
| Actin, gamma1 | ACTG1 | NP_001605 | 42 | 210 |
| Actin, beta | ACTB | NP_001092 | 42 | 10 |
| Coronin 1C | CORO1C | NP_055140 | 54 | 49 |
| Beta tubulin | TUBB | NP_821133 | 50 | 10 |
| Protein regulator of cytokinesis 1 | PRC1 | NP_003972 | 71 | 39 |
| Gelsolin | GSN | NP_000168 | 86 | 6 |
| Flightless-I homolog | FLII | NP_002009 | 146 | 11 |
| Flotillin 1 | FLOT1 | NP_005794 | 47 | 3 |
| Vacuolar protein sorting protein 16 | hVPS16 | NP_072097 | 95 | 3 |
| Epithelial protein lost in neoplasm | EPLIN | NP_001107018 | 86 | 37 |
| NCK interacting protein with SH3 domain | NCKIPSD/WISH | NP_057537 | 80 | 8 |

**Table S1. TEM4-interacting proteins.** Accession numbers, predicted size (kDa), and peptide count (total) of all proteins that co-immunoprecipitated with GFP-TEM4 in HeLa cells identified by mass spectrometry. Conditions of mass spectrometry have been described (Ngok et al., 2012).